

1 **Electronic Supplementary Information**

2 **Pt nanospheres grown paper working electrode based electrochemical device for** 3 **in-situ and real-time determination of the flux of H₂O₂ releasing from SK-BR-3** 4 **cancer cells**

5 Fang Liu^a, Shenguang Ge^b, Jinghua Yu^{a,*}, Mei Yan, Xianrang Song^c

6

7 **Materials and methods**

8 **Reagents**

9 All chemicals and solvents used here were aseptic after heat sterilization
10 treatment. Chloroplatinic acid (H₂PtCl₆) was obtained from Shanghai Chemical
11 Reagent Company (Shanghai, China). Catalase (from bovine liver, lyophilized
12 powder, 2000-5000 U/ mg, Sigma), phorbol myristate acetate (PMA, ~99%, Sigma),
13 N-formylmethionyl-leucylphenylalanine (fMLP, ≥97%, Sigma), adenosine 5'-
14 diphosphate (ADP, ≥95%, Sigma), ascorbic acid (AA, ≥99.0%, Sigma), Solutions
15 of H₂O₂ were freshly diluted from the 30% solution, and their concentrations were
16 determined using a standard KMnO₄ solution. The S6 aptamer with high specificity
17 for SK-BR-3 cells was synthesized and purified by Shanghai Sangon Biotechnology
18 Co. Ltd. (Shanghai, China).

19 The human breast cancer cells SK-BR-3 were provided by Shandong Tumor
20 Hospital. The sequence of S6 aptamer was 5'-NH₂-TGGATGGGGAGAT
21 CCGTTGAGTAAGCGGGCGTGTCTCTCTGCCGCCTTGCTATGGGG-3'. Calcein

22 acetoxymethyl ester (AM) and fluorescein isothiocyanate labeled annexin-V (FITC-
23 annexin-V) were purchased from Beijing Biosynthesis Biotechnology Co. Ltd.
24 (Beijing, China).

25 0.1 M phosphate buffer solution (PBS, pH 7.4) was employed as the supporting
26 electrolyte. Carbon ink (ED423ss) and Ag/AgCl ink (CNC-01) were
27 purchased from Acheson. Whatman chromatography paper #1 (58.0 cm × 68.0 cm)
28 (pure cellulose paper) was obtained from GE Healthcare Worldwide
29 (Pudong, Shanghai, China) and used with further adjustment of size (A4 size).

30 **Apparatus**

31 Scanning electron microscope (SEM) analyses were performed using QUANTA
32 FEG 250 thermal field emission scanning electron microscopy (FEI Co., USA).
33 Electrochemical impedance spectra (EIS) were performed on a CHI 604D
34 electrochemical workstation (Shanghai CH Instruments Inc., China). Electrochemical
35 measurements were carried out with a homemade EC system. The current was
36 measured on a CHI 660D electrochemical workstation (Shanghai Chenhua Apparatus
37 Corporation, China) with a three-electrode system, whereas the modified PWE with a
38 diameter of 6.0 mm was used as the working electrode, screen-printed carbon
39 electrode and Ag/AgCl electrode were used as the counter electrode and the reference
40 electrode, respectively.

41 **Preparation of Pt nanoparticles**

42 Pt nanoparticles were prepared according to a facile method described as follows.
43 H_2PtCl_6 and trisodium citrate solutions were filtered through a 0.22- μm microporous

44 membrane filter prior to use, and then 3.0 mL of 1% trisodium citrate was added to 20
45 mL of boiling 0.05% H₂PtCl₆ solution and stirred for 30 min at the boiling point. The
46 final Pt nanoparticles prepared by this method have an average diameter of ~5 nm.

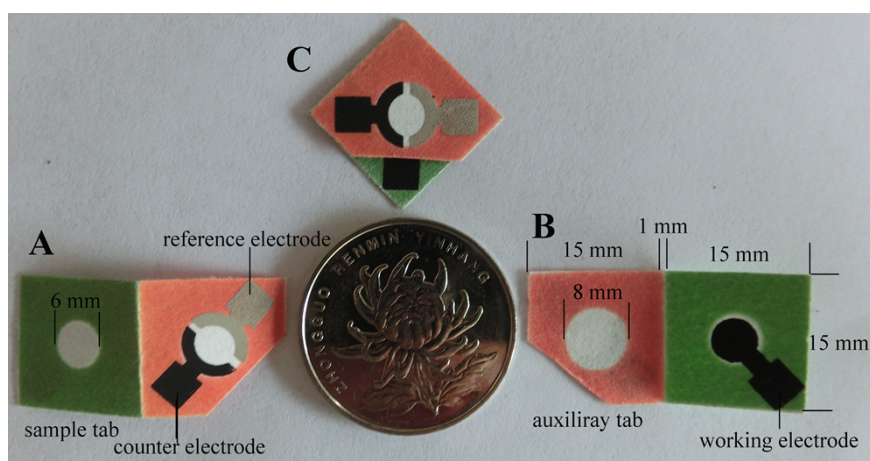
47 **Fabrication of Pt-PWE**

48 Prior to the S6 aptamer immobilization, growth of Pt layer on the surfaces of
49 cellulose fibers in the paper working zone of PWE was implemented to fabricate a
50 novel Pt-PWE with enlarged effective surface area and enhanced electrocatalytic
51 reduction property for sensitive H₂O₂ sensing. This novel Pt-PWE was fabricated on
52 this 3D origami electrochemical device through a direct chemical reduction of
53 H₂PtCl₆ by AA. First, as-prepared Pt nanoparticle seeds solution (15.0 μL) was
54 dropped into the bare PWE. Then the origami device was equilibrated at room
55 temperature for 1 h to optimize the surface immobilization of Pt nanoparticle seeds on
56 cellulose fibers. After rinsing with water thoroughly to remove loosely bound Pt
57 nanoparticle seeds, freshly prepared silver-growth solution (15.0 μL) containing
58 0.50 mM H₂PtCl₆ and 0.25 mM AA was applied into the Pt nanoparticles seeded
59 PWE, respectively, and incubated at room temperature for 4 min. During the growth
60 process, the Pt nanoparticle seeds acted as catalysts for the reduction of H₂PtCl₆ by
61 AA, resulting in the enhancement of the Pt nanoparticle seeds. Subsequently, the
62 resulting Pt-PWEs were washed with water thoroughly. Thus a layer of
63 interconnected Pt nanoparticle on cellulose fibers with good conductivity was
64 obtained (Scheme 1B), which was dried at room temperature for 20 min.

65 **Cell culture**

66 The SK-BR-3 human breast cancer cells were obtained from Shandong Tumor
67 Hospital. Breast cancer cells were maintained in dulbecco's modified eagle medium
68 (DMEM) supplemented with 10% fetal bovine serum and 1% penicillin/streptomycin.
69 Cultures were maintained at 37 °C and in 5% CO₂ atmosphere. The culture medium
70 was changed every other day and the cells were passaged when they reached 80-90%
71 confluency. For cancer cell electrochemical measurement, cells were placed inside a
72 12-well plate. When cultured for two days, cancer cells were digested by pancreatic
73 enzymes and dispersed in PBS. After being blown well, cancer cells were counted by
74 a Petroff- Hausser cell counter (U.S.A.).

75 **Fabrication and characterization of this 3D origami EC device**



77 Scheme S1. (A) The schematic representation, size, and shape of this μ -PAD. (B) One side of the
78 μ -PAD with the screen-printed reference and counter electrode; (C) The reverse side of (B) with
79 the screen-printed working electrode.

80

81 The preparation of this μ -PAD was similarly to our previous work [1] with large
82 modifications and a detailed procedure was described below. This origami device was

83 comprised of a square sample tab (Scheme S1A, 15.0 mm × 15.0 mm) and a square
84 auxiliary tab (Scheme S1B, 15.0 mm × 15.0 mm). An angle of the square auxiliary tab
85 was cut off for exposure of the contact pad of screen-printed carbon working
86 electrode (Scheme S1B). The entire origami device could be produced in bulk on an
87 A4 paper sheet by a commercially available solid-wax printer (Xerox Phaser 8560N
88 color printer). Owing to the porous structure of paper, the melted wax can penetrate
89 into the paper network to decrease the hydrophilicity of paper remarkably while the
90 unprinted area (paper auxiliary zone and paper sample zone) still maintained good
91 hydrophilicity, flexibility, and porous structure and will not affect the further screen-
92 printing of electrodes and modifications [2].

93 Between the sample tab and auxiliary tab, the unprinted line (1 mm in width)
94 was defined as fold line (Scheme S1B). The unprinted hydrophilic area (paper
95 auxiliary zone and paper sample zone) constituted the reservoir of the paper
96 electrochemical cell (~40 μL) after being folded at the predefined fold line. Then, the
97 wax-penetrated paper sheet was ready for screen-printing of electrode containing the
98 wire and contact pad on its corresponding paper zone (Scheme S1B, C). The electrode
99 array consisted of a screen-printed Ag/AgCl reference electrode and carbon counter
100 electrode on the auxiliary zone (Scheme S1A) and screen-printed carbon working
101 electrode (6 mm in diameter) on the reverse side of paper sample zone (Scheme S1B),
102 respectively. After folding (Scheme S1C), the three screen-printed electrodes will be
103 connected once the paper electrochemical cell was filled with solution.

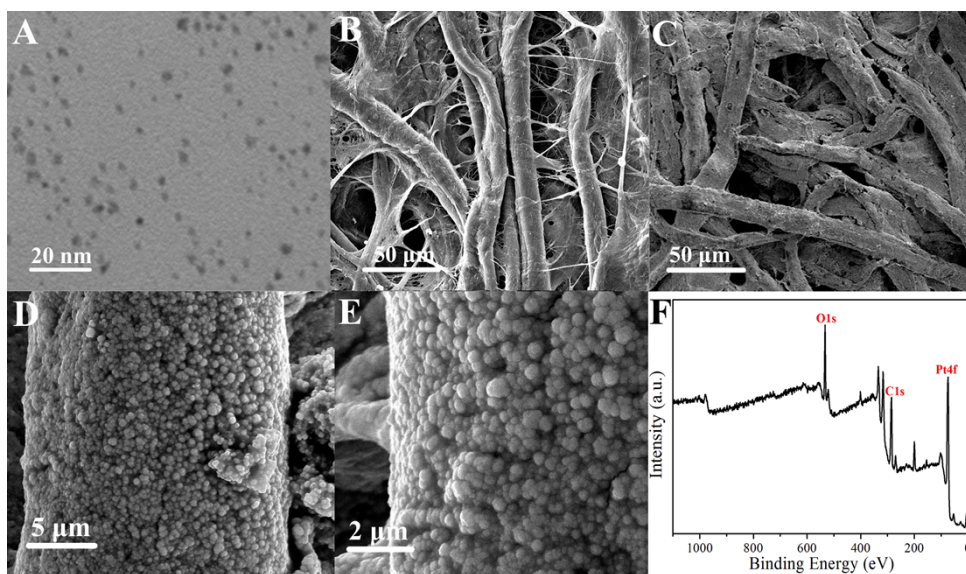
104 **Electrical resistivity of Pt nanospheres grown paper sample zone**

105 To measure the resistivity of Pt nanospheres grown paper sample zone exactly,
106 rectangular paper zones (1.0 mm×20.0 mm) were fabricated by wax-printing and
107 then were modified through the growth of dense Pt nanospheres conducting layer on
108 the surfaces of cellulose fibers in these rectangular paper zones using the same
109 method described in experimental section under the same experimental conditions in
110 each case, the average electrical resistivity of which revealed the electrical resistivity
111 of Pt nanospheres grown paper sample zone in this work. Prior to the measurements,
112 both the bare and Pt nanospheres grown rectangular paper zones were dried in a
113 drying oven for 3 h. Then the measurements were performed with a four-point
114 measurement setup using a digital multi-meter (Agilent, U1251B).

115 **Detection of H₂O₂ standard solution at our cancer cell immobilized Pt-PWE**

116 Our work aimed at developing a biosensor for monitoring the release process and
117 measuring the flux of H₂O₂ from cells. To evaluate the possibility of the biosensor
118 used in this purpose, the current responses of our modified Pt-PWEs toward the
119 various concentrations of H₂O₂ were studied. And the potential swept from 0 to -0.6
120 V with scan rate of 100 mV s⁻¹ after 10 μL of PBS buffer solution (pH 7.4) was added.
121 PBS buffer containing different concentrations of H₂O₂ standard solution (early
122 determined using a standard KMnO₄ solution) were used in this experiment as
123 detection solution. At the absence of H₂O₂, the current response of the modified
124 porous Pt-PWE is weak. Upon addition of H₂O₂ with increasing concentrations, the
125 intensity of the cathodic current of the modified porous Pt-PWE increases gradually.

126 **Characterizations of Pt-PWE**



127 Fig. S1 TEM image of Fig. S1 TEM image of the as-prepared Pt nanoparticle seeds (A); SEM
 128 images of bare paper sample zone of PWE (B); Growth of Pt nanospheres layer on the surfaces
 129 of cellulose fibers in paper sample zone of PWE under different magnification: (C, D, E); XPS of
 130 Pt nanospheres modified paper sample zone (F).

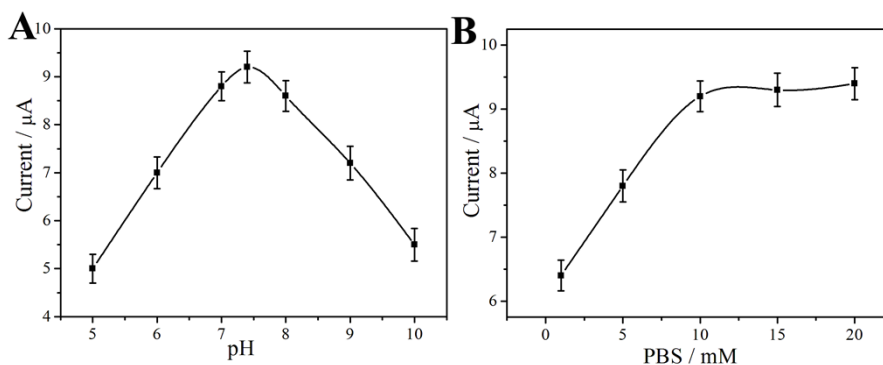
131

132 The PWE was modified through the growth of a Pt nanospheres layer on the
 133 surfaces of cellulose fibers in paper sample zone from Pt nanoparticle seeds to
 134 fabricate this novel Pt-PWE. Fig. 1SA showed the TEM image of the as-prepared Pt
 135 nanoparticle seeds with the average diameter of about 5 nm. As shown in Fig. 1SB,
 136 the porous bare paper sample possessed high ratio of surface area to weight with
 137 rough cellulose fibers, which could offer an excellent adsorption microenvironment
 138 for the Pt nanoparticles. After Pt nanoparticles were successfully seeded and grown
 139 on the cellulose fiber, a continuous and dense Pt nanospheres conducting layer on the
 140 cellulose fiber surfaces was observed (Fig. 1SC, D). The enlarged image of Pt
 141 nanospheres grown cellulose fiber was shown in Fig. 1SE, showing the uniform

142 growth of Pt nanospheres. This indicated that a good coverage of Pt nanospheres on
143 the surfaces of the cellulose fibers was obtained using our simple growth method. The
144 Pt nanospheres grown paper sample zone maintained good 3D interwoven and
145 incompact cellulose fibers networks structure after the growth process, which would
146 facilitate the area-to-volume ratio as well as increase the catalytic active sites to
147 obtain better electrochemical performance. In addition, the successful modification of
148 Pt nanospheres on cellulose fibers was confirmed by X-ray photoelectron
149 spectroscopy (XPS) (Fig. 1SF) and the peaks observed at 73 eV were ascribed to
150 metallic Pt.

151 Optimization of experiment conditions

152 To achieve the optimal analytical properties of the sensing system, pH and ionic
153 strength of assay solution on the sensitivity of the sensor were investigated (Fig. 2S).
154 Fig. 2SA shows the dependence of currents on pH of PBS. An optimal current was
155 obtained at pH 7.4 PBS. A higher or lower pH resulted in the decrease of catalytic
156 currents. In addition, as shown in Fig. 2SB, the current value increased with the
157 increment of ionic strength of assay solution and tended to level off after 10 mM PBS.
158 Thus, a pH 7.4 PBS (10 mM) was chosen as the supporting electrolyte.



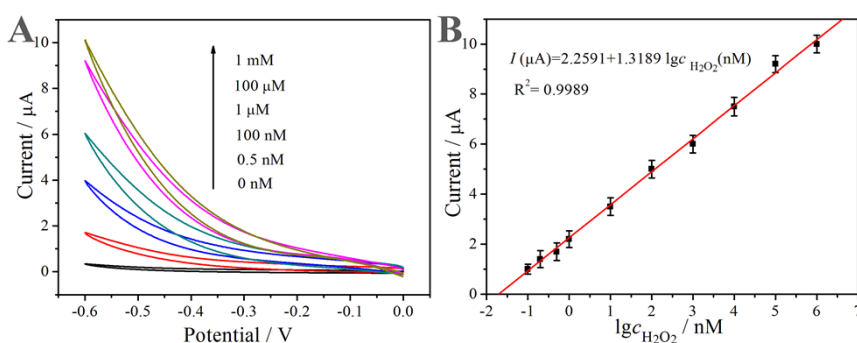
159

160 Fig. 2S Current signal dependence of the Pt-PWE based μ -PADs electrochemical H_2O_2 sensor on
161 (A) different pH of PBS from 5.0 to 10.0; (B) different ionic strength of the assay solution in 1mM,
162 5 mM, 10 mM, 15 mM and 20 mM PBS solution, respectively.

163

164 **The H_2O_2 standard solution concentration-dependent electrocatalytic current**

165 According to the selectivity of results, 10 mM PBS (pH 7.4) was chosen as the
166 supporting electrolyte. Then, under the optimal conditions, our constructed cancer
167 cells immobilized Pt-PWEs were employed to obtain the varied current values
168 towards various concentrations of H_2O_2 (Fig. S3A). The current increased gradually
169 with an increasing concentration of H_2O_2 . When the concentration of H_2O_2 exceeded
170 1.0 mM, the current response became steady (Fig. S3B). The current displays a good
171 linear increase with H_2O_2 in the range 0.10 nM – 1.0 mM, and the calibration equation
172 between the current (I) and the H_2O_2 concentration (c) is expressed as follows: I
173 (μA)= $2.2591+1.3189 \lg c$ (nM), $R^2= 0.9989$.



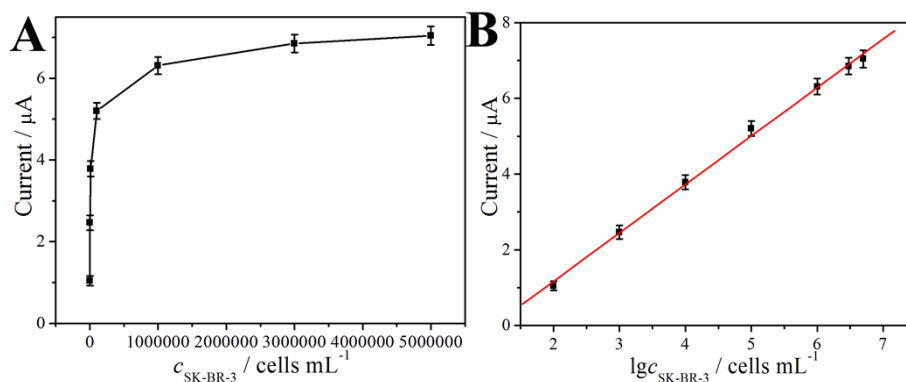
174

175 Fig. S3 The current responses at -0.6 V of the cancer cells immobilized Pt-PWE towards various
176 concentrations of H_2O_2 in 10 mM PBS (pH 7.4) (A); calibration curve for H_2O_2 determination (B).

177

178 **The cell concentration-dependent electrocatalytic current**

179 Under the optimal conditions, we also have investigated the influence of the cell
180 concentration on the electrode to the electrical signal of the releasing H₂O₂. And our
181 modified Pt-PWEs were incubated with various concentrations of SK-BR-3 cells.
182 Subsequently, cells were stimulated by PMA (100 mg mL⁻¹), and the varied current
183 responses were recorded in Fig. S4. The current increases gradually with an
184 increasing concentration of SK-BR-3 cells (Fig. S4A) and the current displays a good
185 linear increase with the logarithm value of cell concentration cells H₂O₂ in the range
186 of 1×10² to 5×10⁶ cells mL⁻¹ (Fig. S4B). The linear relation is not applicative when
187 the cell concentration exceed 5×10⁶ cells mL⁻¹. As cell is a nonconductive
188 biomacromolecule and may obstruct electron transfer and mass trans-port of the
189 electrochemical probe. The calibration equation between the current (*I*) and the H₂O₂
190 concentration (*c*) is expressed as follows: I (μA)= -1.3935+ 1.2795 lg $c_{\text{SK-BR-3}}$ (cells
191 mL⁻¹), R²= 0.9987.



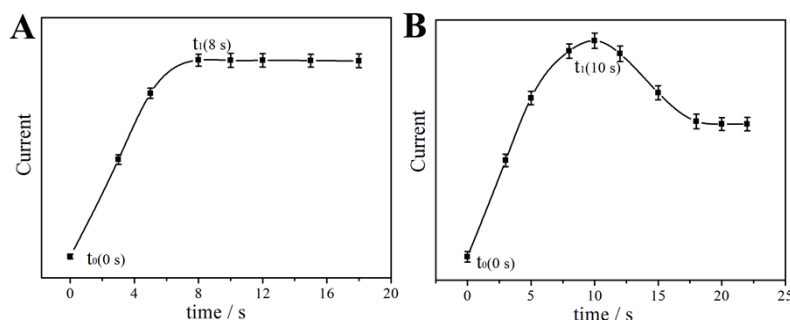
192

193 Fig S4 Relationship between current and SK-BR-3 cells concentration, each point is the average
194 of five measurements (A); logarithmic calibration curve for SK-BR-3 cells (B).

195

196 **Current analysis of the flux of H₂O₂ releasing from SK-BR-3 cells**

197 Information on the mechanism of H₂O₂ release from cells can be inferred from
198 the time-current response. The H₂O₂ determination was measured at different time
199 after the PMA buffer was added to the cancer cells immobilized Pt-PWE. As shown
200 in Fig. S5A, the current increased with the time varying from t₀ to t₁, demonstrating
201 that a short period is needed for cancer cells to be stimulated completely. Then a
202 stable current reached featuring the end of the event. So our H₂O₂ determination was
203 measured after t₁ (8 s), so as to obtain the stable and accurate current value.



204

205 **Fig. S5** The time-current response of H₂O₂ released from cancer cells induced by 100 ng mL⁻¹
206 PMA based on our cancer cells immobilized Pt-PWE (A) and Pt nanospheres modified ordinary
207 glassy carbon electrode (B).

208 As a comparison, Pt nanospheres modified ordinary glassy carbon electrode was
209 applied for the determination of the flux of H₂O₂ releasing from SK-BR-3 cells. To
210 achieve the electrochemical measurements, a conventional three electrode system was
211 constructed: a modified glassy carbon electrode as the working electrode, Pt and
212 Ag/AgCl electrode were used as the counter electrode and reference electrode,
213 respectively. 2.0 mL of PBS solution containing PMA (100 mg mL⁻¹) was used as
214 determination and stimulation buffer and time-current course was recorded in Fig.

215 **S5B**. It can be observed that the trend was similar to that of the curve in **Fig. S5A** with
 216 the time varying from t_0 to t_1 . The current reduces gradually to a lower value beyond
 217 the time t_1 (10 s) due to the diffusion process of H_2O_2 released from SK-BR-3 cancer
 218 cells. The diffusion process of H_2O_2 lower the determination accuracy, and this can be
 219 largely improved by using our cancer cells immobilized Pt-PWE. It can be explained
 220 that our Pt nanospheres **grown** paper sample zone maintained good 3D interwoven
 221 and incompact cellulose fibers networks structure, allowing cells to adhere (highly
 222 affinitive binding with aptamers) to the cellulose fibers to achieve the in-situ and real-
 223 time determination of extracellular H_2O_2 (as shown in Scheme 1D). Only 10 μ L of
 224 buffer is needed to the Pt-PWE, so H_2O_2 can be electrocatalyzed adequately when
 225 releasing from cancer cell and rarely diffuse away. Based on the above, our designed
 226 cancer cell immobilized Pt-PWE demonstrates some advantages in accuracy and
 227 sensitivity of H_2O_2 determination. **To further confirm the superiority of our H_2O_2**
 228 **biosensors, analytical performance of some other H_2O_2 biosensors has been collected**
 229 **in Table S1. As shown in Table S1, our strategy shows shorter response time and**
 230 **lower detection limit than other H_2O_2 assays as reported previously.**

231

232 **Table S1. Comparison analytical performance of some H_2O_2 biosensors**

H_2O_2 biosensor	Response time /s	Detection limit / μ M	Reference
HRP-Au colloid-cysteamine	15	0.58	[3]
nitrogen-doped graphene	20	0.05	[4]
HRP-Nafion-silica-sonogel-carbon	35	1.6	[5]

Pt grown paper working electrode	8	0.0001	This work
----------------------------------	---	--------	-----------

233

234 **References**

235 [1] J. Lu, S. Ge, L. Ge, M. Yan, J. Yu, *Electrochim. Acta.*, 2012, **80**, 334.

236 [2] E. Carrilho, A. W. Martinez and G. M. Whitesides, *Anal. Chem.*, 2009, **81**, 7091.

237 [3] Y. Xiao, H. X. Ju, H. Y. Chen, *Anal. Biochem.*, 2000, **278**, 22.

238 [4] P. W, Z. W. Cai, Y. Gao, H. Zhang, C. X. Cai, *Chem. Commun.*, 2011, **47**, 11327.

239 [5] M. Elkaoutit, I. Naranjo-Rodriguez, M. Domínguez, M. P. Hernández-Artiga, D. Bellido-Milla,

240 J. L. H. H. de Cisneros, *Electrochim. Acta.*, 2008, **53**, 7131.

241